1. The citation (kçe et al. 2021) is present in the text, but reference is missing in the reference section. Could you please provide the reference or delete the text citation?

Correct citation should be: Gökce et al. 2021

2. The reference: (Gökçe et al. 2021) is present in the reference section but not in the text. Could you please check?

Correct citation in the text has been added. This is the same as AQ1.

Rapid electrical impedance detection of sickle cell vaso-occlusion in microfluidic device

Springer Nature or its licensor (e.g. a society or other partner) holds exclusive rights to this article under a publishing agreement with the author(s) or other rightsholder(s); author self-archiving of the accepted manuscript version of this article is solely governed by the terms of such publishing agreement and applicable law.

Yuhao Qiang Affiliationids : Aff1

Darryl Dieujuste Affiliationids : Aff1

Jia Liu Affiliationids : Aff1

Ofelia Alvarez Affiliationids : Aff2

E Du⊠

Email: edu@fau.edu

Affiliationids: Aff1, Correspondingaffiliationid: Aff1

Aff1 Department of Ocean and Mechanical Engineering, Department of Biological Sciences Department of Ocean and Mechanical Engineering, Florida Atlantic University, 33431, Boca Raton, FL, USA

Aff2 Division of Pediatric Hematology and Oncology, University of Miami, 33136, Miami, FL, USA

Abstract

Sickle cell disease is characterized by painful vaso-occlusive crises, in which poorly deformable sickle cells play an important role in the complex vascular obstruction process. Existing techniques are mainly based on optical microscopy and video processing of sickle blood flow under normoxic condition, for measuring vaso-occlusion by a small fraction of dense sickle cells of intrinsic rigidity but not the vaso-occlusion by the rigid, sickled cells due to deoxygenation. Thus, these techniques are not suitable for rapid, point-of-care testing. Here, we integrate electrical impedance sensing and Polydimethylsiloxane-microvascular mimics with controlled oxygen level into a single microfluidic chip, for quantification of vaso-occlusion by rigid, sickled cells within 1 min. Electrical impedance measurements provided a label-free, real-time detection of different sickle cell flow behaviors, including steady flow, vaso-occlusion, and flow recovery in response to the deoxygenation-reoxygenation process that are validated by microscopic videos. Sensitivity of the real part and imaginary part of the impedance signals to the blood flow conditions in both natural sickle cell blood and simulants at four electrical frequencies (10, 50, 100, and 500 kHz) are compared. The results show that the sensitivity of the sensor in detection of vaso-occlusion decreases as electrical frequency increases, while the higher frequencies are preferable in measurement of steady flow behavior. Additional testing using sickle cell simulants, chemically crosslinked normal red blood cells, shows same high sensitivity in detection of vaso-occlusion as sickle cell vaso-occlusion under deoxygenation. This work enables point-of-care testing potentials in rapid, accurate detection of steady flow and sickle cell vaso-occlusion from microliter volume blood specimens. Quantification of sickle cell rheology in response to hypoxia, may provide useful indications for not only the kinetics of cell sickling, but also the altered hemodynamics as obseved at the microcirculatory level.

Keywords

Sickle cell disease
Hypoxia
Electrical impedance
Vaso-occlusion
Microfluidics

Supplementary Information

1. Introduction

Vaso-occlusion is responsible for a variety of clinical complications in sickle cell disease (SCD) such as pain crises, pulmonary hypertension, stroke, and end-organ damage. Evidence also indicates that vaso-occlusion is the likely etiology of sudden death among individuals with sickle cell trait who engage in competitive sports under extreme physical exertion (Harris et al. 2012). The defective gene responsible for SCD leads to abnormal hemoglobin S (HbS) in a patient's red blood cells (RBCs), also known as sickle cells, which are stiffer and stickier than normal RBCs. In addition, HbS in sickle cells polymerizes into rigid fibers when exposed to low oxygen tension, causing misshaped RBCs with significantly reduced cell deformability. Vaso-occlusion process is known to be multifactorial (Francis and Johnson 1991), where leukocyte adhesion, vascular intimal hyperplasia and fat embolism act as prerequisites, and trapping of poorly deformable sickle cells may ultimately result in obstruction of small blood vessels and stop the blood flow. During this process, timing is critical for most of sickle cells escaping the narrow capillaries before they become rigid enough to get trapped (Higgins et al. 2007). Hence, rapid cell sickling constitutes an important risk factor for painful vaso-occlusion.

Clinical management of SCD requires patient self-monitoring of pain events and decreasing stress as suggested by the US Centers for Disease Control and Prevention (Chuang and Demontis 2021). For patients with SCD, it is essential that care providers also monitor for clinical signs and avoid factors such as temperature change or dehydration which could impact on vaso-occlusive pain. However, clinical monitoring and pain assessments are subjective and unquantifiable (Gillis et al. 2012). Existing laboratory techniques for SCD monitoring used in clinical settings include the quantitation of HbS and HbF by different laboratory methods, which require sophisticated equipment, special reagents and complicated procedures (Chen et al. 2012). Growing efforts have been made in developing affordable point-of-care devices, such as a high-throughput screening assay based on detecting the ability of RBCs to traverse a column of tightly packed Sephacryl chromatography beads (Pais et al. 2009), and a paper-based colorimetric assay which can qualitatively differentiate SCD blood from sickle cell trait and normal blood using the blood stain patterns, as well as sensors for monitoring oxygen saturation levels in blood (Yang et al. 2013).

In the laboratory setting, introducing oxygen tension control to microfluidics has enabled in vitro cell sickling measurement via microscopic analysis, from the sub-cellular level to the whole blood level, such as the deformability measurement of cellular membrane (Qiang et al. 2019), microfluidic assays for bio-rheological characteristics of sickle RBC suspension (Higgins et al. 2007; Wood et al. 2012) and single RBCs detection of HbS polymerization in deoxygenated liquid drops (Abbyad et al. 2010), investigation of pathologic adhesion in blood rheology (Tsai et al. 2011), and image flow cytometry to detect morphologic characteristics of deoxygenated RBCs (Van Beers et al. 2014). Furthermore, combination of on-chip oxygen control and capillary-like structures into microfluidic platform has enabled direct measurements of cell deformability and capillary obstruction by rigid, sickled cells rapidly within minutes (Du et al. 2015). Importantly, quantifications of the interactive mechanism between the cell sickling and biorheology in response to hypoxia may provide useful indications of vaso-occlusion and disease severity (Wood et al. 2012; Du et al. 2015).

Moving away from the expensive data acquisition and analysis for cell sickling kinetics and vaso-occlusion testing has been a challenge because these in vitro approaches require microscopic images and videos, which are not suitable for rapid, point-of-care testing. To overcome these limitations associated with optical detection, electrical impedance sensing is advantageous in its label-free nature and high flexibility in configuration and integration into microfluidic channels, which has opened a variety of applications for flow cytometry (further insights refer to reviews (Daguerre et al. 2020); AQ1 kee et al. 2021) and detailed biophysical characterization, such as in cancer cells (Feng et al. 2019). These studies showed that any changes in subcellular components, cell surface area and volume can contribute to the measurable impedance signals for cell distinction. Similar modifications to RBCs, associated with cell sickling events, have inspired us to integrate electrical impedance sensing into microfluidics with on-chip oxygen control for rapid measurements of single sickle cells in flow (Liu et al. 2018) and cell sickling kinetics in suspensions (Liu et al. 2019). As the widespread availability of microcontrollers and smartphones have further opened new avenues for point-of-care microfluidic electrical biosensors (Zarei 2017; Zhao et al. 2020), we further developed an Arduino-based portable impedance measurement device that is compatible with narrow microfluidic channels for single sickle cell impedance analysis (Dieujuste et al. 2021). Recently, a study (Man et al. 2021) reported a development on electrical impedance measurement of vaso-occlusion by chemically treated RBCs and sickle cells at atmospheric oxygen tension environment. The gradient capillary structure is advantageous in processing large volume of blood specimens, but a long term (~ 20 min) perfusion is needed to generate a measurable impedance signal from the capillary obstructions. This technique is limited in detection of the occlusion induced by presence of rigid sickle cells or chemically stiffened RBCs and maybe further developed to test vaso-occlusion attributed by the cell sickling events due to HbS polymerization process.

In this paper, we demonstrate a proof-of-concept of an electrical impedance-based measurement of sickle cell vaso-occlusion in Polydimethylsiloxane (PDMS) microfluidic mimics of capillary structures. The method is innovative in that it can simulate the dynamic changes in the sickle cell rigidity and microrheology from the low oxygen tension induced HbS polymerization, as occur in vivo. The device consists of a double-layer microfluidic capillary structure, embedded with microslit array, and an integrated electrical impedance sensor, allowing real-time rheological measurement that is specific to sickle blood. Cell sickling events attributed capillary obstructions are observed within less than 20 s, facilitating a rapid vaso-occlusion testing (wihtin 1 min). A full rheological transition from steady flow, vaso-occlusion, to flow recovery in response to a brief (70 s) deoxygenation-reoxygenation process is detected in sickle blood cells. Robustness in the impedance detection of vaso-occlusion is confirmed using both natural sickle cells and sickle cell simulants. Performance evaluation of the device at frequencies between 10 and 500 kHz suggests the feasibility of further miniaturization and portability of the entire system, by replacing the benchtop impedance measurement device with a portable device that operates up to 100 kHz (Dieujuste et al. 2021), thus facilitating its application in the finger prick-based blood testing at point-of-care settings.

2. Experimental

2.1. Sample preparation

Normal blood and sickle cell blood samples were obtained with the Institutional Review Board (IRB) approvals by Florida Atlantic University and the University of Miami. All samples were stored at 4 °C and tested within one week of collection. Prior to each experiment, blood samples were washed twice with phosphate-buffered saline (PBS) at the speed of 2000 rpm at room temperature for two minutes. A total of seven blood conditions were tested, including normal RBCs, sickle RBCs from a sickle cell patient, treated with and without anti-sickling agent, 5-hydroxymethyl-2-furfural (5-HMF), as well as five sickle cell simulants. 5-HMF treatment to sickle cells was conducted by incubating blood with 5 mM 5-HMF for 60 min at 37 °C in 1.5 ml Eppendorf tubes. The treated cells were washed twice with PBS to remove the residual drug before the measurement. For all testing, the hematocrit was adjusted to be 0.1% by resuspending 1 µL RBC pellet into 1 mL PBS. Then the cell suspension was injected into the microfluidic channel using a 1 mL syringe with a 23-gauge blunt needle for impedance measurement. In the case of sickle cell simulants, 1% glutaraldehyde dissolved in PBS was added to the flow of normal blood cells, which crosslinked cell membranes and reduced cell deformability, thus leading to vaso-occlusion.

2.2. Experimental setup

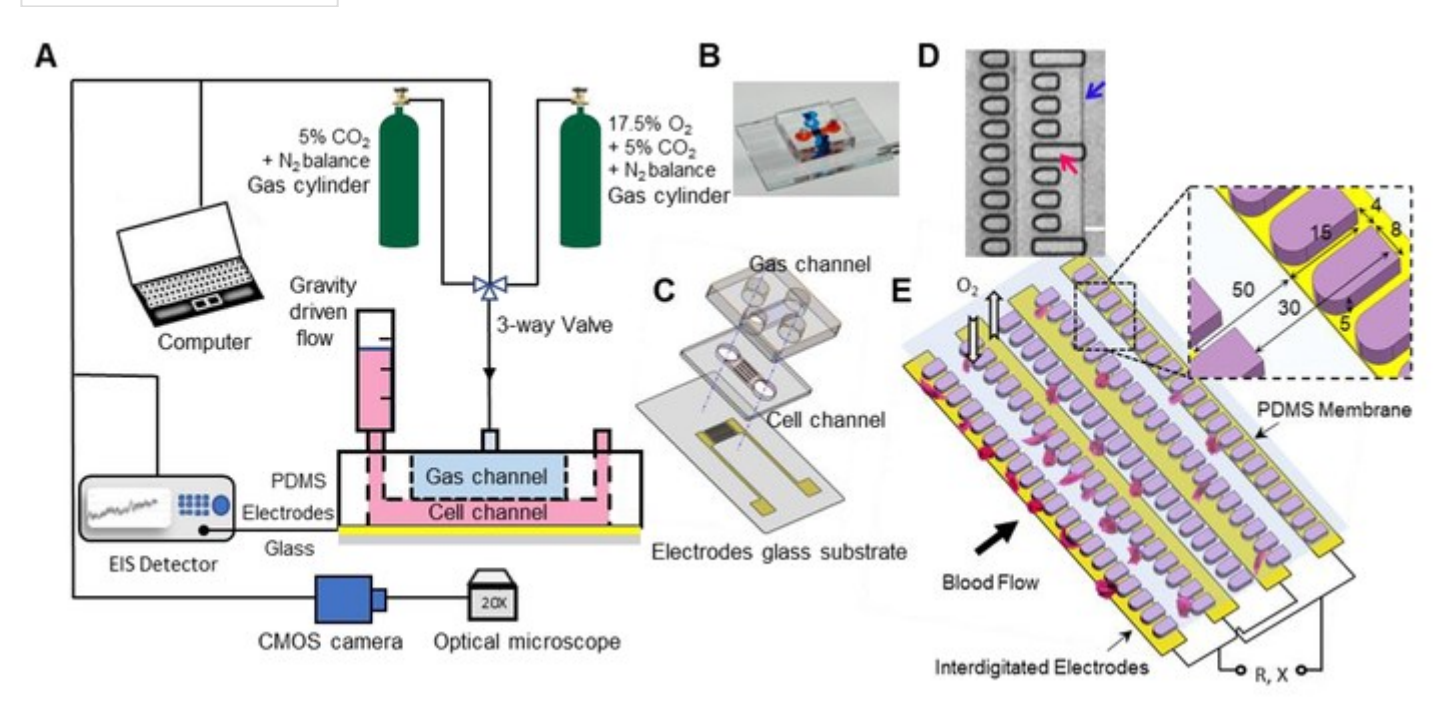
Figure 1 A shows a schematic diagram of the overall experimental setup. Gravity-driven flow approach was used to drive blood flow, by connecting the cell channel to the external hydraulic columns via flexible Tygon microbore tubing (0.020 " ID × 0.060 " OD). An equivalent pressure difference (~ 500 Pa) was utilized throughout the flow experiment. The microfluidic device consists of a PDMS double-layer microchannel for oxygen control and a thin-film (100 nm) interdigitated indium-tin-oxide (ITO) electrodes for impedance sensing (Ossila Ltd, UK) (Fig. 1 B and C). ITO electrodes of excellent transparency were selected to validate the electrical impedance results through simultaneous optical microscopy of microslit obstruction by rigid cells. The interdigitated electrode array consists of 3 pairs of fingers with 100 μm band and 50 μm gap, well aligned to the intersectional area of the double-layer PDMS channels for optimal signal-to-noise ratio. The interdigitated electrodes were soldered by copper-based wires on its soldering pads using the conductive epoxy adhesive (MG Chemicals, ON, CA). With the aid of a stereo microscope, we fully overlaid and carefully aligned the micro-slits to be perpendicular to the interdigitated microelectrode arrays (Fig. 1 D). Permanent covalent bonding was created between the PDMS channel and the glass substrate using air plasma cleaner (Model PDC-001, Harrick Plasma) for 1 min.

To demonstrate the capability of electrical impedance in the real time sensing of the dynamic flow behaviors of sickle cells, microfluidic devices with 4 µm micro-slits were used. Blood flow of sickle cells treated with and without 5-HMF were tested and compared to the flow of normal blood. During the testing, blood samples were injected into the microfluidic channel and flow was created by hydrostatic pressure. A gas control system was used to create a dynamic hypoxia environment that can rapidly induce a scenario of blood flow variations, such as cell sickling events for the vaso-occlusion testing. Oxygen level in the cell channel was controlled by gas diffusion through a 150 µm thick PDMS layer at 4.5 psi. Gas mixtures included a high oxygen concentration (17.5% oxygen, 5% carbon dioxide with the balance of nitrogen) and a low oxygen concentration (5% carbon dioxide with the balance of nitrogen). A programmable 3-way valve through uProcess scripting software (LabSmith., CA, USA) was used to switch between the two gas supplies as shown in Fig. 1 A, allowing us to create a dynamic gas environment of sickle blood flows. Figure 1 E shows the schematic of the detailed microfluidic design in the cell channel with capillary-inspired structures from our previous development (Du et al. 2015). The micro-slits were able to trap sickle cells once they become rigid and allow only the deformable ones to squeeze through.

Fig. 1

Experimental setup for the proof-of-conception of the microfluidic assay for rapid, electrical impedance measurement of sickle cell vaso-occlusion. (A) A schematic of the complete experimental setup. (B) A photograph of the microfluidic device. (C) Exploded view showing the three components of the microfluidic device, including the gas channel, cell channel and the electrode glass chip. (D) A representative microscopic image showing the alignment of the microstructures (denoted by the red arrow) perpendicular to the ITO electrodes (denoted by the blue arrow). Scale bar: 10 μm. (E) Schematic of the core part of the cell channel with capillary-inspired structures over the interdigitated electrodes. The inset shows the dimensions of the micro-slits

Click here to Correct



Testing of the blood flow of sickle cell simulants wasere conducted using microfluidic devices with 6 µm micro-slits. This was because RBCs became rigid and lost their deformability immediately after encountering glutaraldehyde in the microfluidic channel, thus failed to

enter the channel of 4 μ m micro-slits. During the testing, the microfluidic device was initially primed with PBS and flow was created by hydrostatic pressure. Then a 10 μ L volume was withdrawn and discarded from the inlet and replaced with 10 μ L of diluted RBCs. After visually confirmed the cells entering the micro-slits under microscope, a 10 μ L was withdrawn and replaced with 1% glutaraldehyde.

Impedance measurement of blood flow was made with a commercial EIS HF2IS (Zurich Instruments, AG, Switzerland), using an AC signal ofat 2 V_{pk} at frequencies of 10 kHz, 50 kHz, 100 and 500 kHz, respectively. Impedance signals were acquired at a sampling rate of 7 data points per second. All the impedance results are normalized by measuring relative increases in the real part of impedance, ΔR and the negative of the imaginary part of impedance, ΔX , to the initial value of the measurement per each cell condition. Blood flows were recorded using a CMOS camera at a frame rate of 10 frames per second (The Imaging Source, Charlotte, NC), which is mounted on an Olympus X81 inverted microscope (Olympus America, PA, USA). Image contrast was enhanced by inserting a 414 \pm 46 nm band pass filter in the optical path. All tests were performed at room temperature.

2.3. Oxygen level control

Oxgen concentrations in the microfluidic device were calibrated offline using a fiber-optic O_2 microsensor (Pyroscience GmbH, Aachen, Germany) connected to a Firesting O_2 fiber-optic meter and controlled by Pyro Oxygen Logger software (Pyroscience GmbH, Aachen, Germany) (Fig. 2A). The microfluidic device was flipped, where the gas channel was bonded to the glass substrate while the cell channel was exposed. Detailed structure of the microfluidic chip was described by the exploding view and cross-sectional view by Fig. 3B and C, respectively. This allowed the microprobe of the O_2 sensor to be easily inserted into the gas channel and cell channel (Fig. 2A inset) for O_2 measurement. To simulate the blood testing conditions, the cell channel was filled with PBS and the gas channel was supplied by gas mixture, switching between the high and low O_2 levels and maintained at low and high O_2 levels for 60 s and 10 s, respectively. The actual O_2 concentration in the cell channel varied between 15.9% and 0.5% when the O_2 level varied between 17.1% and 0.4% in the gas channel. A complete deoxygenation-reoxygenation cycle was 70 s. Figure 2D demonstrates the results of O_2 concentration profiles in the gas channel and cell channel during a 3-consecutive deoxygenation process.

Fig. 2

Oxygen concentration calibration within the microfluidic device. (A) A photograph of the experimental setup. The inset shows the schematic of the oxygen sensor probe inserted into the cell channel of the microfluidic device. Exploded view (B) and Sectional view a-a (C) showing the multiple layers of the microfluidic device used for O_2 sensing. (D) O_2 concentration profiles measured in the gas channel and cell channel during a cyclic deoxygenation-reoxygenation process

Click here to Correct

2.4. Microscopic analysis of blood flow

Microscopic video of blood flow was recorded simultaneously with the electrical impedance measurement for validation. The time lapse video was analyzed using ImageJ/Fiji (Schindelin et al. 2012). Blood flow condition was quantified by cell fraction, CF, the overall area blocked by the cells in the field of view of the micro-slits. Blood flow of normal blood, sickle blood treated with and without 5-HMF was evaluated from 4 consecutive measurements per cell condition, expressed as mean \pm SD. Blood flow of each sickle cell simulant was evaluated by a single testing, as the chemically cross-linked cell membrane is irreversible. Custom MATLAB script was developed to directly compare the time-dependent data between microscopy and impedance of blood flows.

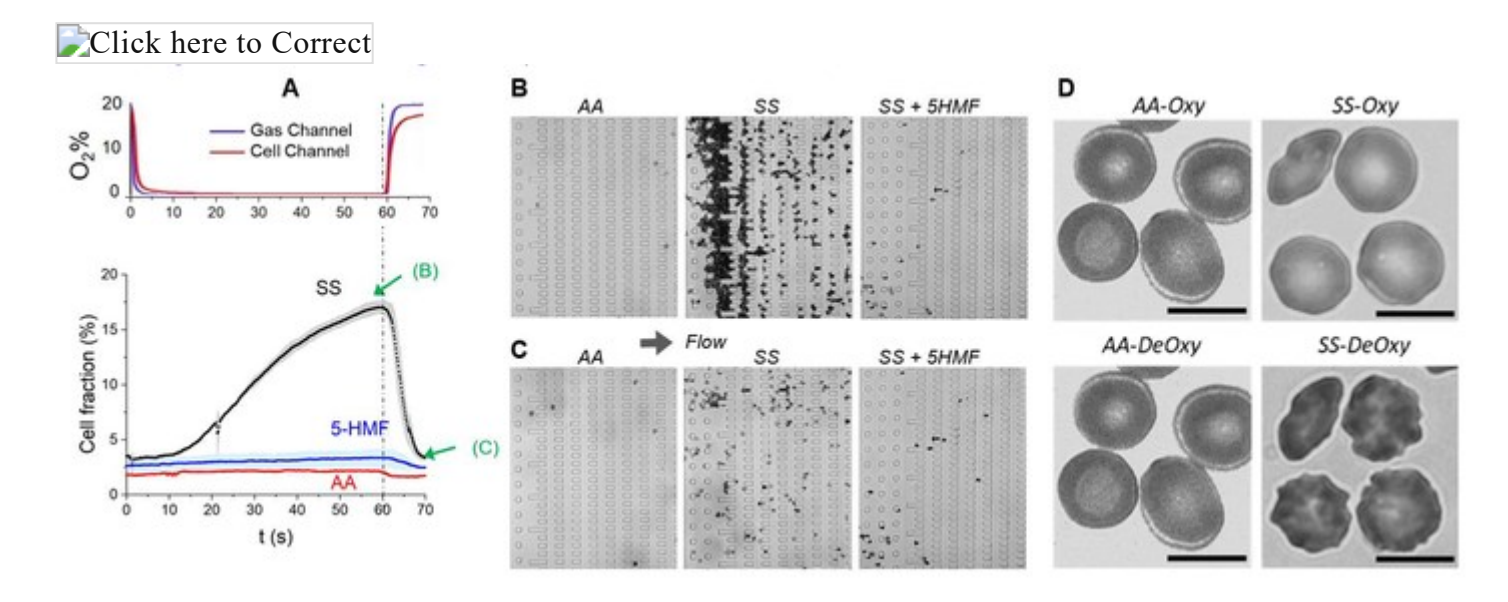
3. Results and discussion

3.1. Deoxygenation-induced vaso-occlusion in sickle blood

A short term (60 s) of deoxygenation is found to be sufficient to differentiate flow of sickle cells from normal RBCs as well as sickle cells treated with anti-sickling agent (Fig. 3). When sickle blood is subjected to transient hypoxia, including a rapid deoxygenation, fully deoxygenation, and rapid reoxygenation, a dynamic change in flow behavior, including steady flow, vaso-occlusion, and flow recovery was observed (Fig. 3B). Vaso-occlusion procedure is quantified by the time series data of cell fraction in the microfluidic channel by optical microscopy. Cell fraction value of sickle blood flow changes drastically in response to the 70-s reoxygenation-reoxygenation, including an initial steady flow phase (0–10 s), a vaso-occlusion phase (10–60 s), and a flow recovery phase (60–70 s) (Fig. 3A lower panel, black curve, supplementary video 1). During the initial 10 s of deoxygenation, oxygen concentration in the cell channel quickly reduced to a critical level (fully deoxygenated). No apparent occlusion occurs in sickle cells due to the delay time in HbS polymerization. During the vaso-occlusion phase, cell sickling events continue, resulting in rigid, sickled cells being trapped by the micro-slits. Due to the flow condition, more sickle cells flow into the deoxygenation site, causing more cell sickling events and additional occlusion till a peak is reached at the 60 s. Immediately, a reoxygenation is made, due to rapid dissolution of sickle hemoglobin polymers, sickled cells resume their deformability and the blood flow recover to the original level. In contrast, normal RBCs showed no apparent occlusion through the measurement, which was associated with relatively stable cell fraction values, regardless of variations in oxygen levels (Fig. 34 A lower panel, red curve). Similar result is found in sickle cells treated by 5-HMF, which is known to have beneficial anti-sickling effect on sickle cells by improving their oxygen affinity of hemoglobin (Abdulmalik et al. 2005; Zhao et al. 2013; Hannemann et al. 2014). (Fig. 3A lower panel, blue curve). Representative microscopic images of blood flow conditions at two different time points (peak of vaso-occlusion and flow recovery in sickle cells) are shown in Fig. 34B and C. Through the simultaneous optical microscopy, we verify that most of the trapped cells in sickle blood flow are sickled, which show marked morphological changes (shape and roughness) due to intracellular HbS polymerization as opposed to those normal RBCs (Fig. 3D), consistent to a prior study (Du et al. 2015).

Fig. 3

Microscopy of blood flow in the microfluidic device. (A) Cell fraction value as a quantitative measurement of blood flow condition in response to deoxygenation-reoxygenation, achieved by gas perfusion in normal RBCs (AA – red curve), sickle RBCs (SS - black curve), and sickle RBCs treated with 5-HMF (5-HMF – blue curve). Solid curve represents the mean value and shade represents the standard deviation obtained from four consecutive measurements of each cell condition. (B) and (C) Representative microscopic images (cropped) of blood flow conditions at time points as indicated by (B) and (C) in the bottom panel of (A). Blood flows from left to right. (D) Representative microscopic images showing morphological characteristics of AA and SS RBCs under oxygenation (upper panel) and deoxygenation (lower panel), respectively. Scale bar is 10 μm



3.2. Electrical impedance detection of changes in blood flow behavior

The principle of electrical impedance analysis of blood flow is based on the shifts in the measured reactance and resistance signals, resulting from the interactions of the flowing cells with the sensing electrodes in the microfluidic channel when other parameters are unchanged. Figure 4 AB shows the electrical equivalent circuit model of a suspension of cells, adapted from references (Seoane et al. 2004; Qiao et al. 2012). At low frequencies, current flows primarily through intercellular spaces in the device due to the insulating cell membranes (Fig. 4A), therefore the relative change in the measured impedance value provides a label-free measurement of the cell concentration (or the extent of vaso-occlusion) within the cell channel. According to the cell equivalent circuit model where cell membrane capacitance is connected in series to the electrode capacitance, a reduction in the system capacitance or an increase in the negative of the reactance is expected as sickled cells are gradually trapped at the micro-slits. We mainly investigated the cell behaviors at low frequencies (< 1 MHz) in the β -dispersion of cell suspensions (Asami 2002) due to interfacial polarization, mainly attributed to the capacitive plasma membranes. As electrical impedance provided a real-time measurement of the microfluidic channel system for its overall opposition to alternating currents, which depends on the microfluidic channel, cell concentration, and flow rate etc. Herein, we intended to measure the changes in the impedance signals caused by the change of cell concentration within a fixed region during the vaso-occlusion process. To quantify the varied flow conditions, we calculated the relative change in the time series of impedance signals with respect to the initial data point, R_0 and X_0 at t = 0 as reference values per cell condition,

$$\Delta R = R - R_0$$

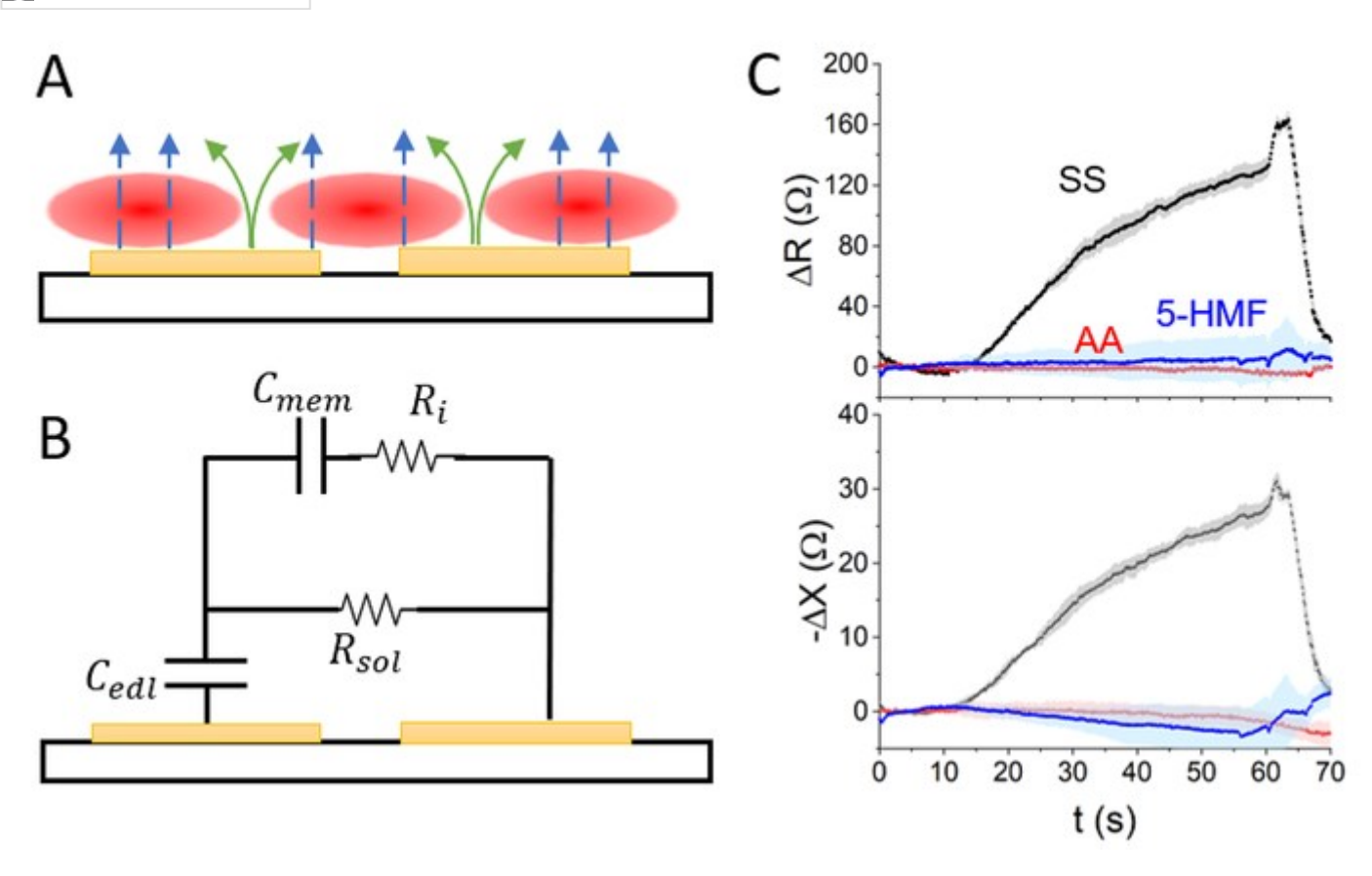
$$\Delta X = X - X_0$$

where R is the real part, resistance, and X is the imaginary part, reactance of the impedance. This relative measurement is found to provide repeatable and accurate results of all flow conditions, while eliminates the potential influence of inter-device variations as well as the almost unavoidable time shift in impedance sensing, although the latter was found to be minor during a short-term testing.

Figure 4 C shows the representative impedance signals measured at 10 kHz for sickle blood. The time-series of impedance signals, including both the real part, ΔR and negative of the imaginary part, -ΔX, show good conformity to the cell fraction values (Fig. 3A). A stable impedance signal implies a steady blood flow, and a variation in the impedance signal implies an altered rheology, such as an occlusive process by rigid, sickled cells in response to deoxygenation or a flow recovery when the trapped cells are released due to reoxygenation. This suggests that both parts of the impedance signals could be used to detect vaso-occlusion. Changes in the impedance signals caused by the sickle cell vaso-occlusion is found to be similar to the behavior of cell suspensions, such that the reactance values decrease with the increase of cell impedance in the suspension of endothelial cells (Liu et al. 2010), and the electrical impedance increased as cell concentration increases within a fixed region of cell suspension of yeast cells (Soley et al. 2005). However, we observe that ΔR provides a more accurate measurement of steady flow than the imaginary part, -ΔX, especially for the steady flow behavior as observed in blood flow of normal RBCs and drug-treated sickle cells (red and blue curves). This implies that the real part of the impedance signals is less susceptible to deoxygenation process. In addition, impedance signals of sickle blood increase sharply at 60 s, which is believed to be associated with the variations in the system, e.g., the disturbed fluid volume upon gas valve switching. Importantly, consistency in impedance measurement of different flow behaviors is observed across all frequencies (See supplementary information, Fig. S1).

Impedance measurement of vaso-occlusion in sickle cell blood. (A) Diagram of blood suspension within a shallow channel modelled as a layer of cells in contact with electrodes. Blue dashed arrows represent high frequency electric current and green arrows represent low frequency electric current. (B) The electrical equivalent circuit model of cell suspension. The cell membrane and interior are equivalent to a capacitance, C_{mem} and a resistance R_i in series due to their electrical characteristics. The surrounding solution is equivalent to a resistance R_{sol} . The electrical double layer is equivalent to an electrode capacitance, C_{edl} . (C) Representative electrical impedance measurement (10 kHz) of altered blood flow behavior in sickle cells under a transient hypoxia, and nearly steady flow behaviors in normal blood and sickle blood treated with anti-sickling agent regardless of oxygen tension. Solid curves show the mean value of impedance data and shades show the standard deviation for normal RBCs (AA, red curve), sickle RBCs (SS, black curve), and treated sickle RBCs treated (5-HMF, blue curve)

Click here to Correct

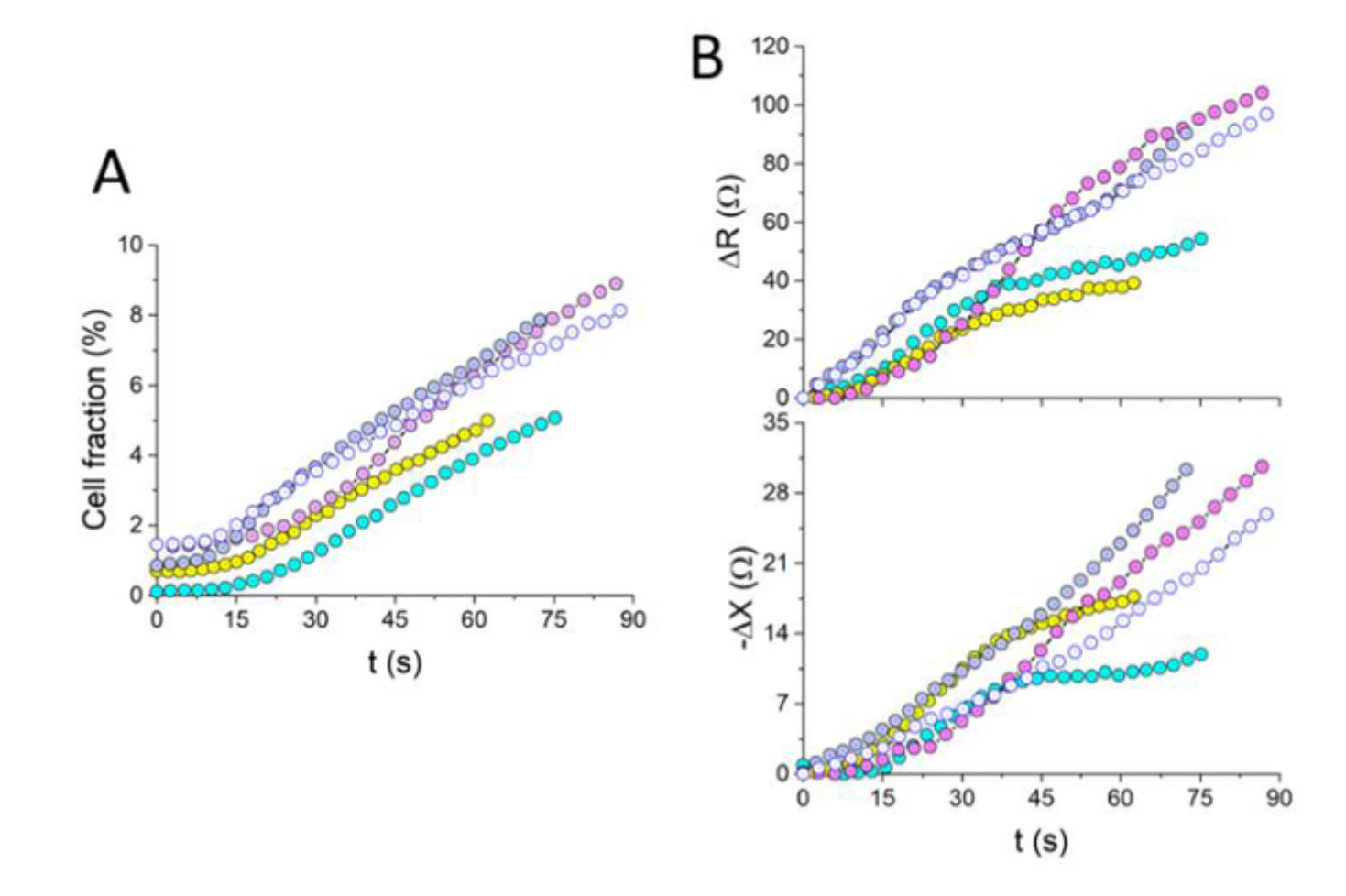


To assess the robustness in impedance detection of vaso-occlusion in potentially heterogenous sickle cell samples, we adjust parameters for sickle cell simulant, such as the time of adding glutaraldehyde to the normal blood flow and duration of measurement (60–90 s), resulted in different occlusion fractions and occlusion rates (Fig. 5A). Representative impedance data at 10 kHz is shown in Fig. 5B. Both the real part and imaginary part of impedance are found to be useful in detection of occlusion by rigid sickle cell simulants, similar to the impedance detection of sickle cell vaso-occlusion. A greater change in impedance value corresponds to a bigger change in cell fraction value. It is noted that such consistency across all testing frequencies is only identified in the real part of impedance (See supplementary information, Fig. S2). More noise is found in the imaginary part of the impedance at higher frequencies, implying the real part is less susceptible to other factors in the circuit system.

Fig. 5

Impedance measurement of vaso-occlusion in sickle cell simulant. (A) Cell fraction value of blood flow in five sickle cell simulants, each represented by a different color. (B) Representative impedance signals for detection of vaso-occlusion, as quantified by ΔR and ΔX at a representative frequency, 10 kHz, following the same color code as cell fraction measurement

Click here to Correct



3.3. Sensitivity of impedance in response to vaso-occlusion

Sensitivity of electrical impedance in detection of vaso-occlusion is assessed by the relative change in electrical impedance versus ΔCF , the relative change in the cell fraction value with respect to the initial value, CF₀. We compared the time-dependent responses of vasoocclusion, ΔCF based on 4 and 6 μm micro-slit devices. For sickle cell vaso-occlusion, data at 20, 26, 30, 40, and 60 s per cycle are extracted from the time-series measurements to have a distribution over the range of vaso-occlusion. For sickle cell simulants, data at 30 s, 60 s, and the time point with maximum vaso-occlusion are extracted. It can be seen from Fig. 6 that when the vaso-occlusion of sickle cells increases from 2.6 to 13.5%, the sensor response at 10 kHz increases from 15 Ω to 121 Ω and 15 Ω to 60 Ω for resistance ΔR and reactance $-\Delta X$, correspondingly. Similar sensor response to vaso-occlusion of sickle cell simulants is observed. When vaso-occlusion increases from 2 to 6.1%, the sensor response at 10 kHz increases from 19.5 Ω to 40.9 Ω and 7.1 Ω to 14.6 Ω for resistance ΔR and reactance $-\Delta X$, correspondingly. Sensor response is highly frequency dependent. We calculate the sensitivity from the slope with a linear fit of the response at each frequency. As shown in Table, sensitivity decreases with electrical frequency. In addition, sensitivity of R is much higher than that of reactance X across all frequencies, regardless of the dimension of micro-slit. Marked variations in the sensitivity of reactance is observed for 6 µm micro-slit and at higher testing frequencies. Next, we evaluate the performance of the sensor in steady flow measurement, quantified by the variance of resistance and reactance, respectively. Steady flow is defined as occlusion-free or with negligible occlusion and quantified by the relative change in CF value far below 1%. As sickle cell simulants exhibit vaso-occlusion immediately when cells are in contact with glutaraldehyde, steady flow behavior is evaluated by blood flow of normal RBCs and sickle cells only. For this analysis, blood flow of normal RBCs and 5-HMF treated sickle RBCs during the initial 60 s, as well as blood flow of sickle RBCs during the initial 10 s prior to deoxygenation are included. As shown in Figure 7, variances of both impedance parts decrease with electrical frequency. The variances in the impedance measurements between 50 kHz and 500 kHz are quite close, suggesting that impedance within this range can provide a reliable measurement of steady flow behavior. Considering the overall performance of the impedance in measurement and differentiation between steady flow and vaso-occlusion, we conclude that the real part of the impedance within 50 kHz and 500 kHz is preferable in the current assay.

Table 1
Frequency-dependent sensitivity

Frequency	Sickle cell occlusion (4 μm)		SS simulant occlusion (6 μm)	
	R/CF (Ω/%)	X/CF (Ω/%)	R/CF (Ω/%)	X/CF (Ω/%)
10 kHz	9.6	4.1	11.7	3.8
50 kHz	7.5	1.9	7.1	1.4
100 kHz	6.9	1.6	7.3	0.5
500 kHz	5.5	1.1	7.1	0.2

Fig. 6

Sensitivity of impedance in detection of vaso-occlusion under frequencies of (A) 10 kHz, (B) 50 kHz, (C) 100 kHz, and (D) 500 kHzRed circles are the measurement of occlusion in SS simulants using 6 μ m microslits. Red lines represent the corresponding linear regressions with the shade being the 95% confidence intervals. Black circles are the measurements of occlusion in sickle cells using 4 μ m microslits. Black lines represent the corresponding linear regressions with the shade being the 95% confidence intervals

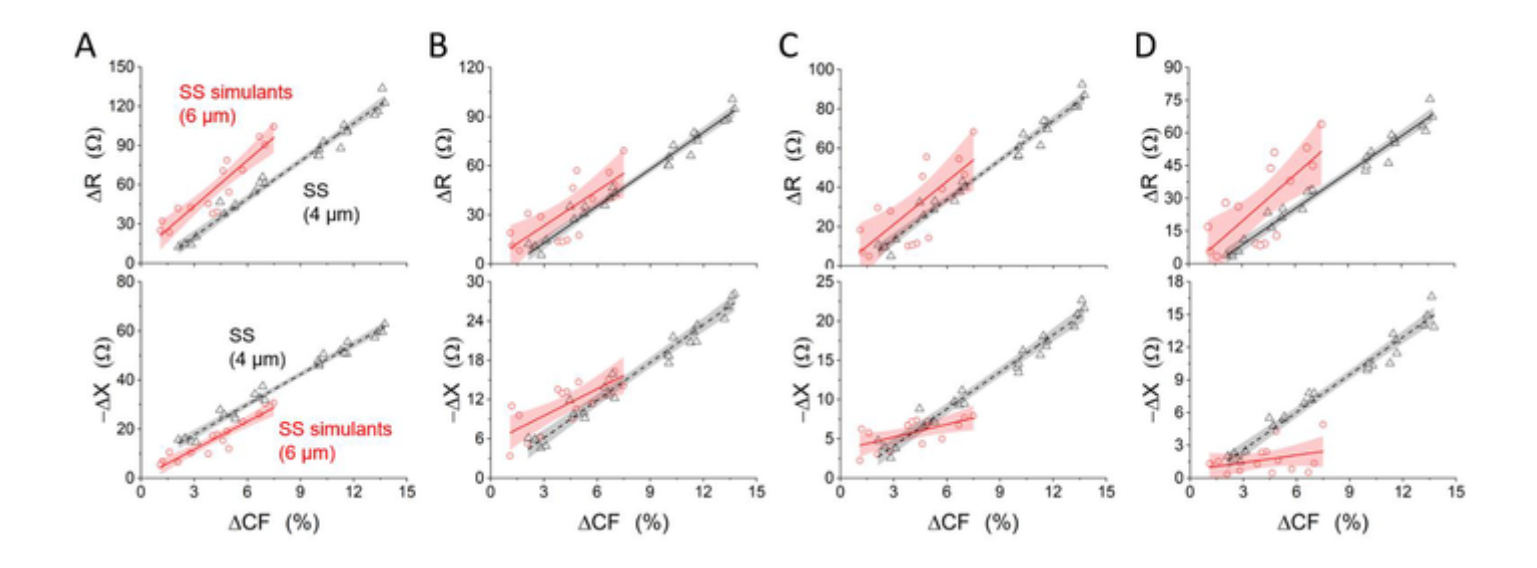
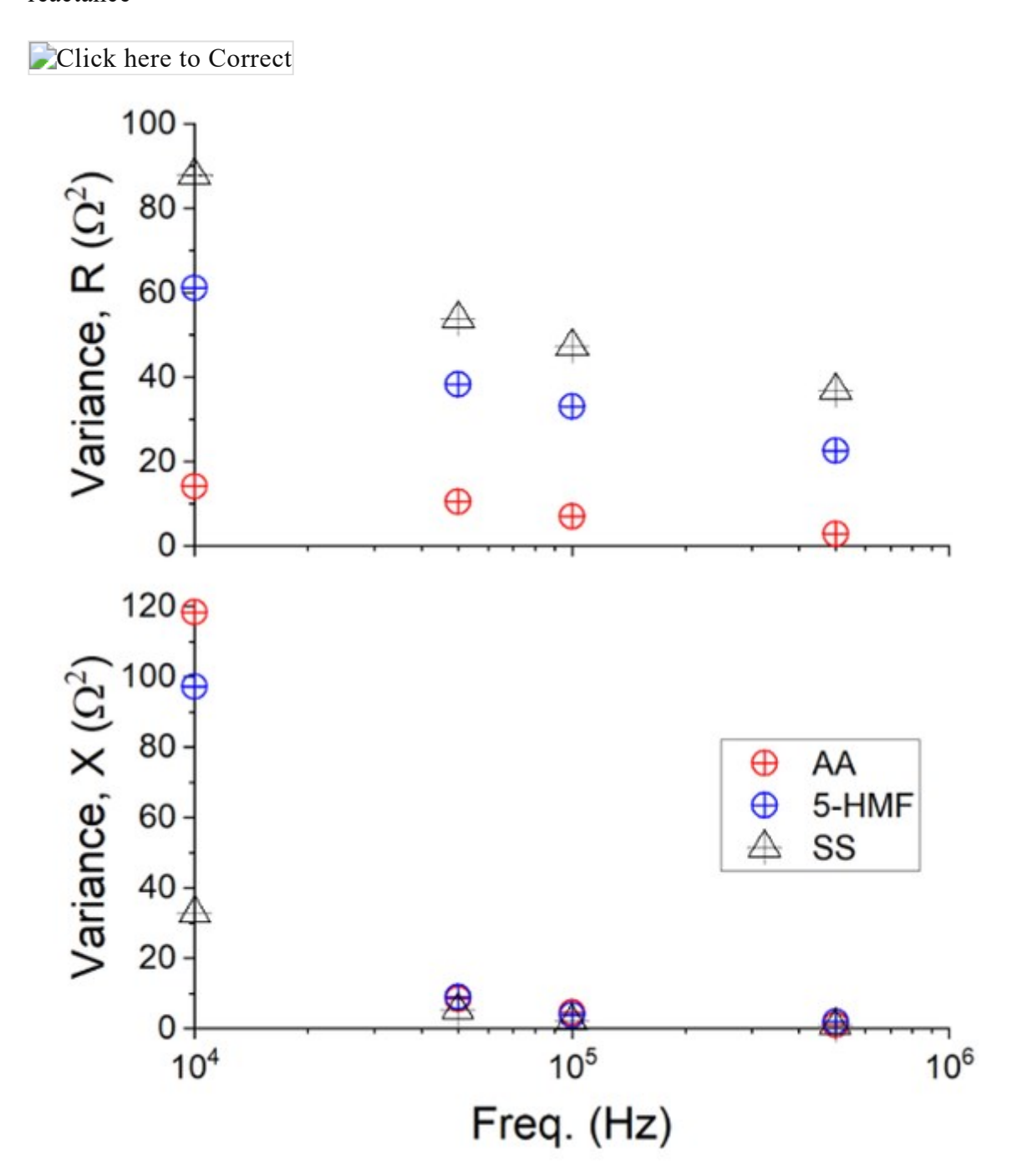


Fig. 7

Frequency-dependence in impedance measurement of steady flow, as quantified by the variance of the relative change in resistance and reactance



4. Conclusions and outlook

The unique feature of the microfluidic assay is the integration of an electrical impedance sensing with the PDMS microfluidic mimics of capillary structure, which enables a label-free, rapid measurement of blood flow behavior and deoxygenation-induced sickle cell vaso-occlusion. The results may provide useful indications of not only the hemodynamics at the microcirculatory level but also alterations due to the kinetic cell sickling events under hypoxia. This developed assay is potentially useful for monitoring blood activities from finger prick blood samples in SCD patients accepting pharmaceutical treatments, such as hydroxyurea (Charache et al. 1996), voxelotor (Vichinsky et al. 2019) d glutamine (Niihara et al. 2018), as well as gene therapies (Demirci et al. 2019). The current proof-of-concept study is limited due to the exclusion of temperature as a dependent factor to the results.

In our future development of next variant of the vaso-occlusion testing for point-of-care use, the gas system will be replaced by pre-coating the cell channel with oxidoreduction reagents, such as glucose oxidase or sodium hydrosulfite (Abbyad et al. 2010), so that rapid cell sickling events can be induced when a drop of blood is directly loaded into the inlet reservoir and flow towards the micro-slits driven by hydrostatic pressure. A fixed frequency, e.g., between 50 and 100 kHz may be selected, in that the benchtop impedance spectroscope will be substituted by an Arduino microcontroller-based portable impedance measurement device (Dieujuste et al. 2021) based on an AD5933 impedance analyzer chip for up to 100 kHz sensing. Temperature can be an important factor that influences the in vitro vaso-occlusion testing, as the rigidity of deoxygenation-induced sickled cells can be much higher at 37 °C than 25 °C (Mackie and Hochmuth 1990). There was also a close correlation between low temperatures and hospital admissions for painful crisis (Redwood et al. 1976). A

comprehensive study on the influence of the environmental temperature on the vaso-occlusion measurement may be necessary to calibrate the in vitro vaso-occlusion measurements for evaluation of the risk of vaso-occlusive pain. Therefore, we envision this blood testing assay can be further developed as a portable system for in situ assessment of abnormal blood flow behavior, serving as peripheral risk factor for painful crisis in sickle cell disease as well as other diseases with altered blood flow behavior.

Publisher's Note

Springer Nature remains neutral with regard to jurisdictional claims in published maps and institutional affiliations.

Acknowledgements

This work was supported by the NSF Grants # 1635312 and # 2032730. Authors D.D. and E.D. acknowledge the support from NIH R01EB025819.

Declarations

Competing Interests There are no conflicts to declare.

Electronic supplementary material

Below is the link to the electronic supplementary material.

Supplementary Material 1

Supplementary Material 2

References

- P. Abbyad, P.-L. Tharaux, J.-L. Martin, C.N. Baroud, A. Alexandrou, Sickling of red blood cells through rapid oxygen exchange in microf luidic drops. Lab. Chip. **10**(19), 2505–2512 (2010)
- O. Abdulmalik, M.K. Safo, Q. Chen, J. Yang, C. Brugnara, K. Ohene-Frempong, D.J. Abraham, T. Asakura, 5-hydroxymethyl-2-furfural modifies intracellular sickle haemoglobin and inhibits sickling of red blood cells. brit. J. Haemat. **128**(4), 552–561 (2005)
- K. Asami, Characterization of biological cells by dielectric spectroscopy. J. Non Cryst. Solids. 305(1-3), 268-277 (2002)
- S. Charache, F.B. Barton, R.D. Moore, M.L. Terrin, M.H. Steinberg, G.J. Dover, S.K. Ballas, R.P. McMahon, O. Castro, E.P. Orringer, Hy droxyurea and sickle cell anemia. Clinical utility of a myelosuppressive "switching" agent. The Multicenter Study of Hydroxyurea in Sic kle Cell Anemia. Medicine. **75**(6), 300–326 (1996)
- T. Chen, R. Lathrop, S. Shevkoplyas, (2012). The case for rapid diagnosis of sickle cell disease: a literature review. J. Glob. Health Persp ect. 2012: 1–7
- C.L. Chuang, F. Demontis, Systemic manifestation and contribution of peripheral tissues to Huntington's disease pathogenesis. Ageing R es. Rev. **69**, 101358 (2021)
- H. Daguerre, M. Solsona, J. Cottet, M. Gauthier, P. Renaud, A.J. Bolopion, (2020). Positional dependence of particles and cells in microfl uidic electrical impedance flow cytometry: Origin, challenges and opportunities. Lab Chip 20(20): 3665–3689
- S. Demirci, A. Leonard, J.J. Haro-Mora, N. Uchida, J.F. Tisdale, CRISPR/Cas9 for Sickle Cell Disease: applications, future possibilities, and Challenges. Cell Biology and Translational Medicine. K. Turksen. Cham. Springer Int. Publishing. **5**, 37–52 (2019)
- D. Dieujuste, Y. Qiang, E. Du, A portable impedance microflow cytometer for measuring cellular response to hypoxia. Biotechnol. Bioen g. **118**(10), 4041–4051 (2021)
- E. Du, M. Diez-Silva, G.J. Kato, M. Dao, S. Suresh, (2015). Kinetics of sickle cell biorheology and implications for painful vasoocclusive crisis. Proc. Natl. Acad. Sci. U.S.A. 112(5): 1422–1427
- Y. Feng, L. Huang, P. Zhao, F. Liang, W.J.A. Wang, (2019). A microfluidic device integrating impedance flow cytometry and electric impedance spectroscopy for high-efficiency single-cell electrical property measurement. Anal. Chem. 91(23): 15204–15212
- R.B. Jr. Francis, C.S. Johnson, Vascular occlusion in sickle cell disease: current concepts and unanswered questions. Blood. 77(7), 1405–1414 (1991)

- V.L. Gillis, A. Senthinathan, M. Dzingina, K. Chamberlain, E. Banks, M.R. Baker, D. Longson, G. Guideline, Development, Management of an acute painful sickle cell episode in hospital: summary of NICE guidance. brit. Med. J. **344**, e4063 (2012)
- AQ2 F. Gökçe, P.S. Ravaynia, M.M. Modena, A. Hierlemann, What is the future of electrical impedance spectroscopy in flow cytometry? Biomicrofluidics. **15**(6), 061302 (2021)
- A. Hannemann, U.M. Cytlak, D.C. Rees, S. Tewari, J.S. Gibson, Effects of 5-hydroxymethyl-2-furfural on the volume and membrane per meability of red blood cells from patients with sickle cell disease. J. Physiol. **592**(18), 4039–4049 (2014)
- K.M. Harris, T.S. Haas, E.R. Eichner, B.J. Maron, Sickle cell trait associated with sudden death in competitive athletes. am. J. Card. 110 (8), 1185–1188 (2012)
- J. Higgins, D. Eddington, S. Bhatia, L. Mahadevan, (2007). Sickle cell vasoocclusion and rescue in a microfluidic device. Proc. Natl. Aca d. Sci. U.S.A. 104(51): 20496–20500
- F. Liu, S. Arifuzzaman, A.N. Nordin, D. Spray, I. Voiculescu, *Characterization of Endothelial Cells Using Electrochemical Impedance Sp ectroscopy* (2010 IEEE APCCAS, IEEE, 2010)
- J. Liu, Y. Qiang, O. Alvarez, E. Du, Electrical impedance microflow cytometry with oxygen control for detection of sickle cells. sens. Act uators B Chem. **255**, 2392–2398 (2018)
- J. Liu, Y. Qiang, O. Alvarez, E. Du, Electrical impedance characterization of erythrocyte response to cyclic hypoxia in sickle cell disease. ACS Sens. 4(7), 1783–1790 (2019)
- L.H. Mackie, R.M. Hochmuth, The influence of oxygen tension, temperature, and hemoglobin concentration on the rheologic properties of sickle erythrocytes. Blood. **76**(6), 1256–1261 (1990)
- Y. Man, D. Maji, R. An, S.P. Ahuja, J.A. Little, M.A. Suster, P. Mohseni, U.A. Gurkan, Microfluidic electrical impedance assessment of r ed blood cell-mediated microvascular occlusion. Lab. Chip. **21**(6), 1036–1048 (2021)
- Y. Niihara, S.T. Miller, J. Kanter, S. Lanzkron, W.R. Smith, L.L. Hsu, V.R. Gordeuk, K. Viswanathan, S. Sarnaik, I. Osunkwo, A phase 3 t rial of l-glutamine in sickle cell disease. N Engl. J. Med. **379**(3), 226–235 (2018)
- E. Pais, J.S. Cambridge, C.S. Johnson, H.J. Meiselman, T.C. Fisher, T. Alexy, A novel high-throughput screening assay for sickle cell dise ase drug discovery. J. Biomol. Screen. **14**(4), 330–336 (2009)
- Y. Qiang, J. Liu, M. Dao, S. Suresh, E. Du, (2019). Mechanical fatigue of human red blood cells. Proc. Natl. Acad. Sci. U.S.A.: 20191033
- G. Qiao, W. Wang, W. Duan, F. Zheng, A.J. Sinclair, C.R. Chatwin, Bioimpedance analysis for the characterization of breast cancer cells in suspension. IEEE. Trans. Biomed. Eng. **59**(8), 2321–2329 (2012)
- A.M. Redwood, E.M. Williams, P. Desal, G.R. Serjeant, Climate and painful crisis of sickle-cell disease in Jamaica. brit. Med. J. 1(6001), 66 (1976)
- J. Schindelin, I. Arganda-Carreras, E. Frise, V. Kaynig, M. Longair, T. Pietzsch, S. Preibisch, C. Rueden, S. Saalfeld, B. Schmid, Fiji: an open-source platform for biological-image analysis. Nat. Methods. 9(7), 676–682 (2012)
- F. Seoane, K. Lindecrantz, T. Olsson, I. Kjellmer, A. Flisberg, R. Bagenholm, *Brain Electrical Impedance at Various Frequencies: The Ef fect of Hypoxia* (Conf Proc IEEE Eng Med Biol Soc, IEEE, 2004)
- A. Soley, M. Lecina, X. Gámez, J. Cairo, P. Riu, X. Rosell, R. Bragos, F. Godia, On-line monitoring of yeast cell growth by impedance sp ectroscopy. J. Biotechnol. **118**(4), 398–405 (2005)
- M. Tsai, A. Kita, J. Leach, R. Rounsevell, J.N. Huang, J. Moake, R.E. Ware, D.A. Fletcher, W.A. Lam, (2011). In vitro modeling of the mi crovascular occlusion and thrombosis that occur in hematologic diseases using microfluidic technology. J. Clin. Invest. 122(1)
- Van E.J. Beers, L. Samsel, L. Mendelsohn, R. Saiyed, K.Y. Fertrin, C.A. Brantner, M.P. Daniels, J. Nichols, J.P. McCoy, G.J. Kato, Imagi ng flow cytometry for automated detection of hypoxia-induced erythrocyte shape change in sickle cell disease. Am. J. Hematol. **89**(6), 59 8–603 (2014)

- E. Vichinsky, C.C. Hoppe, K.I. Ataga, R.E. Ware, V. Nduba, A. El-Beshlawy, H. Hassab, M.M. Achebe, S. Alkindi, R.C. Brown, A phase 3 randomized trial of voxelotor in sickle cell disease. N Engl. J. Med. **381**(6), 509–519 (2019)
- D.K. Wood, A. Soriano, L. Mahadevan, J.M. Higgins, S.N. Bhatia, (2012). A biophysical indicator of vaso-occlusive risk in sickle cell dis ease. Sci. Transl. Med. 4(123): 123ra126-123ra126
- X. Yang, J. Kanter, N.Z. Piety, M.S. Benton, S.M. Vignes, S.S. Shevkoplyas, A simple, rapid, low-cost diagnostic test for sickle cell disea se. Lab. Chip. 13(8), 1464–1467 (2013)
- M. Zarei, Portable biosensing devices for point-of-care diagnostics: recent developments and applications. TrAC Trends Anal. Chem. 9 1, 26–41 (2017)
- L. Zhao, J. Chen, J. Su, L. Li, S. Hu, B. Li, X. Zhang, Z. Xu, T. Chen, In vitro antioxidant and antiproliferative activities of 5-hydroxymet hylfurfural. J. Agric. Food Chem. **61**(44), 10604–10611 (2013)
- W. Zhao, S. Tian, L. Huang, K. Liu, L. Dong, The Rev. Lab-on-PCB biomedical application Electrophoresis. **41**(16–17), 1433–1445 (202 0)